ADVANCED MATERIALS

Experimental

Binary combinations of microspheres used in the experiments described herein involved monodisperse large PS latex particles of (1.28 ± 0.02) μm diameter and small PS latex and silica particles with size ranging from 145 nm to 290 nm. Smaller size PS latex microspheres were prepared by one-stage surfactant-free emulsion polymerization [21] and were purified by dialysis. Larger size PS latex microspheres were obtained using a seeded re-growth procedure [22]. Small silica microspheres were synthesized following Gieshe's approach [23] starting from small ca. 20 nm seeds and re-growing them to the required size. Both larger PS latex and silica microspheres were cleaned by consecutive centrifugation and re-dispersion first in water and then in ethanol. All microspheres were negatively charged with ξ-potentials at pH 5.5 ca. –55 to –60 mV for different silica spheres, –52 mV for small PS latex and –80 mV for 1.28 μm PS latex.

Anhydrous ethanol (Aldrich) was utilized as dispersing solvent with the volume fraction (ϕ_L) of the large polystyrene spheres varied from 1×10^{-2} to 3×10^{-2}, while that of the small spheres (ϕ_S) was in the range of 2×10^{-4} to 2×10^{-3}. Glass slides cleaned in piranha solution and washed with copious amounts of de-ionized water and ethanol were used as substrates for the growth of colloidal crystal film. They were held vertically in the dispersion of microspheres while the ethanol was evaporated at low pressure, typically 45 mm Hg. The typical speed of film formation was 1 cm per 4 to 7 h. Upon ethanol evaporation, convective mass flow and capillary forces cause the microspheres to co-assemble at the air–ethanol–glass interface to form a well-ordered hexagonal close-packed monolayer of large PS spheres decorated with regular arrays of small spheres.

Images were obtained using field emission scanning electron microscopy (FE-SEM) at a low accelerating voltage of 1 kV without the use of a conductive coating.

Received: August 28, 2002
Final version: October 24, 2002

[1] A. van Blaaderen, R. Ruel, P. Wiltzius, *Nature* **1997**, *385*, 321.
[2] K.-H. Lin, J. C. Crocker, V. Prasad, A. Schofield, D. A. Weitz, T. C. Lubensky, G. A. Yodh, *Phys. Rev. Lett*. **2000**, *85*, 1770.
[3] Y. Yin, Y. Xia, *Adv. Mater*. **2002**, *14*, 605.
[4] G. A. Ozin, S. M. Yang, *Adv. Funct. Mater*. **2001**, *11*, 95.
[5] S. M. Yang, H. Miguez, G. A. Ozin, *Adv. Funct. Mater*. **2002**, *12*, 425.
[6] Y. Yin, Y. Xia, *Adv. Mater*. **2001**, *13*, 267.
[7] Y. Xia, G. M. Whitesides, *Angew. Chem. Int. Ed*. **1998**, *37*, 55.
[8] S. H. Park, D. Qin, Y. Xia, *Adv. Mater*. **1998**, *10*, 1028.
[9] S. M. Yang, G. A. Ozin, *Chem. Commun*. **2000**, *24*, 2507.
[10] A. S. Dimitrov, K. Nagayama, *Langmuir* **1996**, *12*, 1303.
[11] P. Jiang, J. F. Bertone, K. S. Hwang, V. L. Colvin, *Chem. Mater*. **1999**, *11*, 2132.
[12] P. A. Kralchevsky, N. D. Denkov, *Curr. Opin. Colloid Interface Sci*. **2001**, *6*, 383.
[13] A. G. Yodh, K.-H. Lin, J. C. Crocker, A. D. Dinsmore, R. Verma, P. D. Kaplan, *Phil. Trans. R. Soc. London A* **2001**, *359*, 921.
[14] P. D. Kaplan, J. L. Rouke, A. G. Yodh, *Phys. Rev. Lett*. **1994**, *72*, 582.
[15] Small microspheres are continuously deposited by the meniscus onto the grown film and their concentration should not increase appreciably at the ethanol–air interface. This is confirmed by an observation that using higher ϕ_S in binary microsphere mixtures results in amorphous films with very disordered large sphere clusters.
[16] K. P. Velikov, C. G. Christova, R. P. A. Dullens, A. van Blaaderen, *Science* **2002**, *296*, 106.
[17] S. Hachisu, S. Yoshimura, *Nature* **1980**, *283*, 188.
[18] M. D. Eldridge, P. A. Madden, D. Frenkel, *Nature* **1993**, *365*, 35.
[19] P. Pieransky, L. Strzelecki, B. Pansu, *Phys. Rev. Lett*. **1983**, *50*, 900.
[20] Y. Yin, Y. Lu, B. Gates, Y. Xia, *J. Am. Chem. Soc*. **2001**, *123*, 8718.
[21] G. T. D. Shouldice, G. A. Vandezande, A. Rudin, *Eur. Polym. J*. **1994**, *30*, 179.
[22] Y. Chung-li, J. W. Goodwin, R. H. Ottewill, *Prog. Colloid Polym. Sci*. **1976**, *60*, 163.
[23] H. Gieshe, *J. Eur. Ceram. Soc*. **1994**, *14*, 205.

Uniform Emulsion-Templated Silica Beads with High Pore Volume and Hierarchical Porosity**

By *Haifei Zhang*, *Georgina C. Hardy*, *Matthew J. Rosseinsky*, and *Andrew I. Cooper**

Materials with hierarchical porosity have attracted much attention recently because they combine the advantages of high surface area with the accessible diffusion pathways associated with macroporous structures. Template synthesis is commonly used for the preparation of ordered microporous and mesoporous materials, e.g., by templating surfactants,[1] colloids,[2] block copolymers,[3] and emulsions.[4] Bimodal pore-size distributions may be obtained by dual templating.[5] Hierarchically porous ordered metal oxides with length scales ranging from 10 nm to several micrometers have been prepared by combining micromolding, colloidal templating, and cooperative assembly of inorganic sol–gel species with a triblock copolymer.[6] Macroporosity (pore diameters > 50 nm) was generated by using colloidal particles or self-assembled nanoparticle building blocks. A simple method involving starch–gel templates and silicalite nanoparticles has been used to fabricate zeolite materials with a hierarchical micro/meso/macroporous structure.[7] Non-ordered macropores in the size range 0.5–50 μm were achieved by varying the amount of starch and the starch/silicalite ratio. Materials with micro/mesoporosity have high surface areas and are important in applications such as catalysis and molecular separations. These materials usually have rather low pore volumes (< 2 cm^3 g^{-1}); higher pore volumes typically arise from large macropores (pore diameters > 1 μm). The inclusion of macropores can provide enhanced mass transport for molecules into and out of the porous structure. This becomes particularly important for large molecules (e.g., polymers, biomolecules) or in viscous systems, where diffusion rates are low.

Macroporous materials are often prepared in the form of continuous monoliths or as thin films. Sometimes particulate materials are preferred because they are easily packed into existing reactors, columns, or fixed beds. Suspension polymerization can be used to prepare large spherical particles, but the particle size distribution is usually broad.[8] Spherical particles with diameters > 500 μm are easily separated by filtration, and are useful in a range of applications. Hard mesoporous silica spheres with diameters in the range 0.1–2 mm were prepared using surfactant-stabilized emulsions, but the particle size distribution was broad and only higher alkoxysilanes such as tetrabutyl orthosilicate were used as the source of silicon.[9] Velev and co-workers have synthesized colloidal-tem-

[*] Dr. A. I. Cooper, Dr. H. Zhang, G. C. Hardy, Prof. M. J. Rosseinsky
Donnan and Robert Robinson Laboratories
Department of Chemistry, University of Liverpool
Crown Street, Liverpool L69 3BX (UK)
E-mail: aicooper@liv.ac.uk

[**] The authors acknowledge The Royal Society for a University Research Fellowship (to AIC) and the Engineering and Physical Sciences Research Council (EPSRC) for financial support (GR/N39999 and GR/R15597)

  0935-9648/03/0101-0078 $ 17.50+.50/0

plated macroporous spherical particles from suspension droplets of close-packed colloidal arrays on a fluorinated oil surface.[10] Ordered millimeter-sized macroporous particles of silica and titania have been fabricated,[11] but it is difficult to generate significant quantities of material by this route. Ruckenstein and Hong developed the technique of 'sedimentation polymerization', whereby aqueous monomer solutions (e.g., acrylamide/*N*,*N*′-methylenebisacrylamide) were injected into a hot oil sedimentation medium.[12] The monomer droplets partially polymerized during sedimentation, and were collected as beads at the bottom of the column. By mixing tetraethyl orthosilicate (TEOS) with the monomer solution, and subsequently calcining the polymer phase, porous silica beads could be obtained.[13] Two kinds of pores were found in the silica beads, the larger pores (around 15 nm) arising from the polymer "porogen". Sedimentation polymerization allows the bead size to be adjusted by utilizing different injection methods or by changing the needle diameter.

We report here a new method for the synthesis of hierarchically porous emulsion-templated polymer/silica composite beads by sedimentation polymerization of a high internal phase emulsion (HIPE).[14] High surface area silica beads were obtained by calcination of the composite structures. This method allows the semi-continuous production of uniform, hierarchically porous silica beads with high pore volumes and interconnected emulsion-templated macropore structures.

Firstly, a TEOS sol was prepared by sonication at 0 °C. The sol was stored at –20 °C for more than 7 days to allow complete hydrolysis of the alkoxy groups.[15] A solution of acrylamide (AM) and a crosslinker, *N*,*N*′-methylenebisacrylamide (MBAM), was then mixed with the TEOS sol at room temperature. Next, an oil-in-water (O/W) HIPE was formed by slowly adding light mineral oil to the aqueous solution while vigorously stirring. The O/W HIPE was then injected as individual droplets into a hot oil sedimentation medium (60 °C). The aqueous phase of the HIPE droplets was partially polymerized during sedimentation. A catalytic amount of a redox co-initiator, *N*,*N*,*N*,*N*-tetramethylethylenediamine (TMEDA), was added to both the internal oil phase and the sedimentation medium to accelerate the free-radical polymerization. After sedimentation, the beads were allowed to remain in the sedimentation column at 50 °C for at least 48 h in order to fully gel the TEOS sol. Spherical crosslinked polyacrylamide (PAM)/silica composite beads were obtained with a relatively narrow size distribution, as shown in Figure 1a.

The HIPE was sufficiently stable during sedimentation to allow rapid polymerization of the continuous monomer phase and to "lock in" the HIPE structure. Figure 1b shows a cross-section of a porous composite bead, and Figure 1c shows the porous bead surface. The emulsion-templated cells are interconnected and open to the bead surface. The surface macropores (0.2–2 μm) are somewhat smaller than the internal macropores, but the overall pore structure is continuous (i.e., there is not an impermeable skin on the bead surface). The total macropore volume (as measured by mercury intrusion porosimetry) was high (5.68 $cm^3\,g^{-1}$) and the degree of porosity was calculated to be 82.1 %. These measurements suggest that the original HIPE structure (about 80 vol.-% internal phase) was completely retained during polymerization. The specific surface area of the beads was found to be 25.0 $m^2\,g^{-1}$ with a micropore surface area of 0.86 $m^2\,g^{-1}$, suggesting that there are very few mesopores or micropores in the composite material.

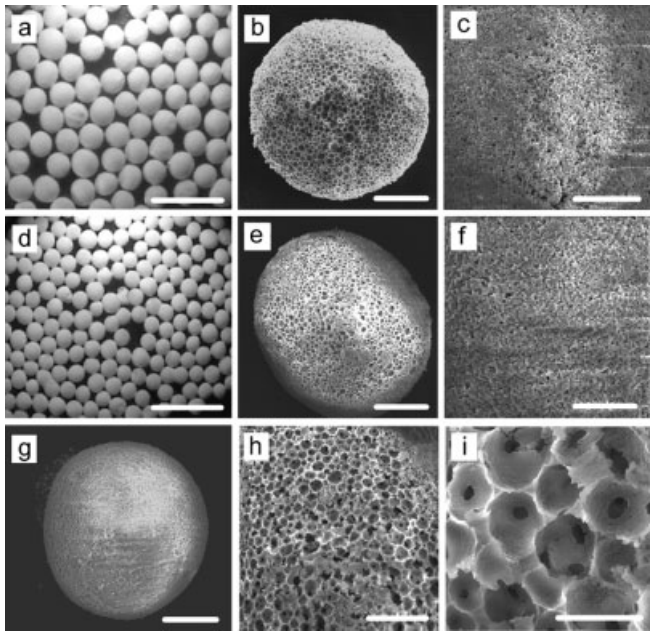

Fig. 1. a–c) Polymer/silica composite beads: a) optical micrograph, scale bar = 5 mm; b) electron micrograph of a single cross-sectioned composite bead, scale bar = 500 μm; c) electron micrograph of the bead surface, scale bar = 100 μm. d–i) Silica beads: d) optical micrograph, scale bar = 5 mm; e) electron micrograph of a single cross-sectioned silica bead, scale bar = 500 μm; f) electron micrograph of the bead surface, scale bar = 200 μm; g) electron micrograph of a single bead, scale bar = 500 μm; h) electron micrograph of porous internal structure, scale bar = 200 μm; i) electron micrograph of porous internal structure, scale bar = 50 μm.

The next step was to remove the polymer phase by calcination. Figure 2 shows a thermogravimetric analysis (TGA) curve for the PAM/silica composite beads under He/O_2. Mass loss continued up to 520 °C, after which the mass remained

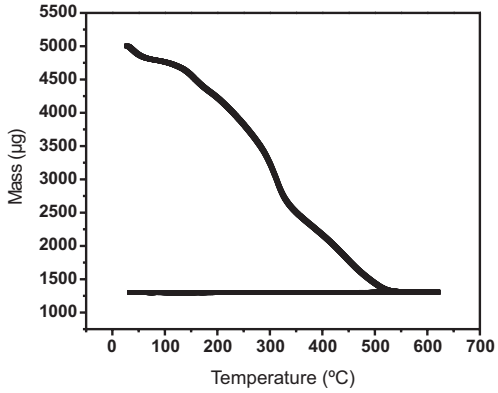

Fig. 2. Thermogravimetric analysis of the polymer/silica composite beads. Program: 1 °C min^{-1} to 600 °C, hold for 30 min, then 1 °C min^{-1} to 20 °C. Gas flow = 350 $cm^3\,min^{-1}$ He + 150 $cm^3\,min^{-1}$ O_2.

  0935-9648/03/0101-0079 $ 17.50+.50/0

ADVANCED MATERIALS

constant. The composite beads were therefore calcined in air at 520 °C for 4 h to yield porous spherical silica beads, as shown in Figure 1d. Before calcination, the average size of the polymer/silica composite beads was 2.00 mm and the standard deviation in bead diameter was 5.1 %. After calcination, the average diameter of the silica beads was 1.34 mm and the standard deviation was 6.1 %, indicating that the composite beads shrank during heating (Fig. 1d). Infrared spectroscopy before and after calcination showed that the PAM carbonyl peak at around 1650 cm^{-1} had completely disappeared. Elemental analysis of the silica beads showed 0.25 % hydrogen and no detectable carbon or nitrogen. (Before calcination, the elemental analysis was: C, 31.05 %; H, 5.84 %; N, 9.75 %). The small amount of residual hydrogen can be attributed to silanol groups.

The electron micrograph in Figure 1e shows the HIPE-templated porous structure of a cross-sectioned silica bead. It can be seen from Figures 1f and 1g that the surface of the spherical silica beads is porous. The internal porous structure of the calcined silica beads is similar to that of the original PAM/silica composite (Figs. 1h and 1i). This is confirmed by the high intrusion volume of the silica beads (5.81 $cm^3\,g^{-1}$ versus 5.68 $cm^3\,g^{-1}$ before calcination). Such complete retention of structure is surprising given that 72 % of the initial mass is lost during calcination. The uniform shrinkage in the materials, and the retention of the macropore structure, suggest that the silica was homogeneously dispersed in the crosslinked polymer (i.e., as a uniform interpenetrating network).[13] The porosity of the silica beads was calculated to be 90.3 % from mercury intrusion porosimetry. This is consistent with the measured bulk density and skeletal density (0.15 $g\,cm^{-3}$ and 2.32 $g\,cm^{-3}$, respectively). The beads were fairly robust when handled carefully, although the mechanical stability was not high. We believe that the mechanical stability could be improved by increasing the ratio of silica sol to organic monomer in the reaction mixture, or by slightly reducing the volume of the HIPE internal phase. Figure 3 shows the macropore size distribution as measured by mercury intrusion porosimetry. The average macropore size for the silica beads (4.85 μm) was smaller than that for the PAM/silica composite beads (11.32 μm) due to shrinkage during calcination.[16]

Mercury intrusion porosimetry only characterizes pores larger than about 7 nm, and the smaller pores in these materials were characterized by gas physisorption analysis. Figure 4 shows N_2 adsorption and desorption isotherms for the silica beads. The adsorption curve rises rapidly in the intermediate zone and shows a hysteresis loop between the adsorption and desorption curves. This behavior is typical for a mesoporous/macroporous material. The specific surface area of the silica beads was calculated to be 421.9 $m^2\,g^{-1}$ using the Brunauer–Emmett–Teller (BET) method. The micropore surface area was found to be 8.9 $m^2\,g^{-1}$. A plot of $dV/d\log(D)$ pore volume versus pore diameter showed a broad peak centered at around 10 nm. X-ray diffraction for the organic/inorganic composite beads before calcining showed a broad, weak peak at $2\theta \sim 0.6°$ (corresponding to *d*-spacing of 14 nm), while the calcined

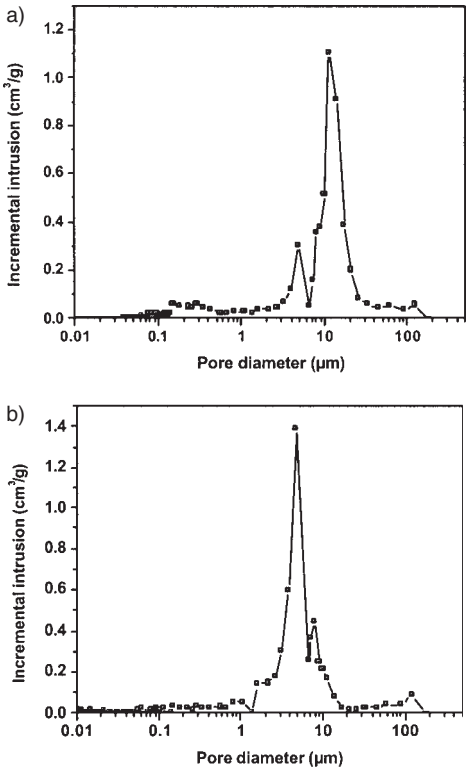

Fig. 3. Pore-size distribution for beads as measured by mercury intrusion porosimetry. a) Silica/PAM composite beads before calcination, peak pore size = 11.32 μm; b) Silica beads after calcination, peak pore size = 4.85 μm.

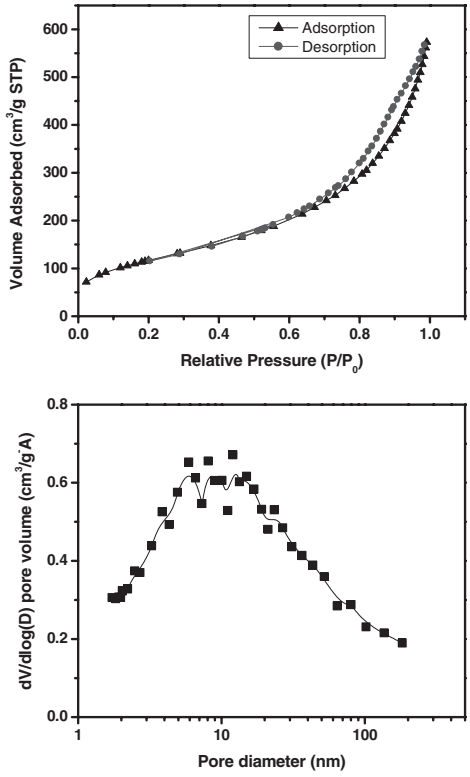

Fig. 4. a) Adsorption and desorption isotherms of silica beads. The BET specific surface = 421.9 $m^2\,g^{-1}$, micropore surface area = 8.9 $m^2\,g^{-1}$. b) Pore-size distribution for silica beads as calculated from adsorption data using Barrett–Joyner–Halenda (BJH) equation.

  0935-9648/03/0101-0080 $ 17.50+.50/0

sample showed a broad asymmetric peak at $2\theta \sim 0.8°$ (a *d*-spacing of 12 nm) that was approximately ten times more intense. This enhanced scattering is consistent with the gas physisorption data, and suggests the generation of mesoporosity that was not present in the samples before calcination.[13,17]

In summary, we have synthesized polymer/silica HIPE-templated porous beads with an average bead diameter of 2.00 mm and high intrusion volume (5.68 $cm^3 g^{-1}$). After calcination, highly porous silica beads were obtained with an average bead diameter of 1.34 mm. The HIPE structure was retained in the silica beads and the material has high surface area (421.9 $m^2 g^{-1}$) and high pore volume (5.81 $cm^3 g^{-1}$). Moreover, our semi-continuous synthetic procedure may, in principle, be scaled up to allow the synthesis of significant quantities of beaded material with a narrow particle size distribution (e.g., by the use of multiple injectors). This new type of silica bead may be useful for applications such as catalysis, biomolecule immobilization, and chromatographic separation. In principle, the method can be extended to prepare a range of materials such as metal and metal oxide porous beads with combined high surface area and high macropore volume.

Experimental

All chemicals were purchased from Aldrich and used as received. The glass sedimentation column was 53 cm in length, had an outside diameter of 5.6 cm, and an internal diameter of 4.6 cm. A mixture of light mineral oil (LMO, 20 vol.-%) and heavy mineral oil (HMO, 80 vol.-%) was used as the sedimentation medium. A redox co-initiator, *N,N,N,N*-tetramethylethylenediamine (TMEDA, 2.5 vol.-%), was added to this medium. The aqueous monomer solution was prepared from acrylamide (15.33 g), *N,N*-methylene bisacrylamide (3.11 g), distilled water (40 cm^3) and poly(vinyl alcohol) (10 000 $g\,mol^{-1}$, 80 % hydrolyzed, 2.25 g). The TEOS sol was prepared by mixing TEOS (33.75 cm^3), distilled water (10.50 cm^3) and 0.9 N hydrochloric acid solution (0.15 cm^3). This mixture was sonicated in an ice–water bath to form a homogeneous solution and then stored at –20 °C before use [15].

The HIPE was prepared as follows: 0.9 N hydrochloric acid solution (1.60 cm^3) was added into the monomer solution (3.0 cm^3) while stirring. The TEOS sol (3.0 cm^3), Triton X-405 (70 % solution 1.4 cm^3), and ammonium persulfate (20 wt.-% solution 0.3 cm^3) were then added. LMO (28 cm^3) containing TMEDA (0.083 g) was added dropwise to this aqueous solution while vigorously stirring. The HIPE was then injected into the sedimentation oil medium at 60 °C using a A-99 FZ Razel syringe pump at a flow rate of 0.5 $cm^3\,min^{-1}$. Droplet sedimentation took 10–20 s. After sedimentation of the HIPE droplets, the partially gelled beads were collected at the bottom of the column. Complete polymerization and gelation of the beads was achieved by heating at 50 °C for at least 48 h. The LMO phase was extracted from the beads by washing with hexane. Calcination of the composite beads was carried out in air using a Carbolite ashing furnace. The temperature was ramped from room temperature to 520 °C at 0.5 °C min^{-1}, held at 520 °C for 4 h, and then cooled to room temperature at 1 °C min^{-1}.

Bead morphologies were investigated with a Hitachi S-2460N scanning electron microscope (SEM). Individual beads were sectioned with a razor blade to reveal the internal structure. Samples were mounted on aluminum studs using adhesive graphite tape and sputter coated with approximately 10 nm of gold before analysis. Intrusion volumes, bulk densities, and macropore size distributions were recorded by mercury intrusion porosimetry using a Micromeritics Autopore IV 9500 porosimeter. Intrusion volumes were calculated by subtracting the intrusion arising from mercury interpenetration between beads (pores > 150 μm) from the total intrusion. The skeletal density was measured using a Micromeritics Helium AccuPyc 1330 pycnometer. Bead surface areas were measured by the BET method using a Micromeritics ASAP 2010 nitrogen adsorption analyzer. Samples were outgassed for 15 h at 90 °C under vacuum before analysis. Thermogravimetric analysis was carried out using a Seiko Instruments Inc EXSTAR 6000, TGA/DTA 6300. X-ray powder diffraction data were collected with Cu Kα1 radiation and a position sensitive detector in capillary transmission geometry using a Stoe Stadi-P diffractometer.

Received: August 14, 2002
Final version: October 14, 2002

[1] a) C. T. Kresge, M. E. Leonowicz, W. J. Roth, J. C. Vartuli, J. S. Beck, *Nature* **1992**, *359*, 710. b) Y. Lu, H. Fan, A. Stump, T. L. Ward, T. Rieker, C. J. Brinker, *Nature* **1999**, *398*, 223.
[2] a) S. A. Johnson, P. J. Ollivier, T. E. Mallour, *Science* **1999**, *283*, 263. b) Y. Xia, B. Gates, Y. Yin, Y. Lu, *Adv. Mater.* **2000**, *12*, 693.
[3] a) P. Yang, D. Zhao, D. I. Margolese, B. F. Chmelka, G. D. Stucky, *Nature* **1998**, *396*, 152. b) D. Zhao, J. Feng, Q. Huo, N. Melosh, G. H. Fredrickson, B. F. Chmelka, G. D. Stucky, *Science* **1998**, *279*, 548.
[4] a) A. Imhof, D. J. Pine, *Nature* **1997**, *389*, 948. b) A. Imhof, D. J. Pine, *Adv. Mater.* **1998**, *10*, 697. c) R. Butler, C. M. Davies, A. I. Cooper, *Adv. Mater.* **2001**, *13*, 1459.
[5] B. T. Holland, L. Abrams, A. Stein, *J. Am. Chem. Soc.* **1999**, *121*, 4308. b) S. A. Davis, S. L. Burkett, N. H. Mendelson, S. Mann, *Nature* **1997**, *385*, 420. c) L. Tosheva, V. Valtchev, J. Sterte, *Microporous Mesoporous Mater.* **2000**, *35–36*, 621.
[6] P. Yang, T. Deng, D. Zhao, D. Feng, D. Pine, B. F. Chmelka, G. M. Whitesides, G. D. Stucky, *Science* **1998**, *282*, 2244.
[7] B. Zhang, S. A. Davis, S. Mann, *Chem. Mater.* **2002**, *14*, 1369.
[8] a) H. G. Yuan, G. Kalfas, W. H. Ray, *J. Macromol. Sci., Rev. Macromol. Chem. Phys.* **1991**, *C31*, 215. b) K. Lewandowski, F. Svec, J. M. J. Fréchet, *Chem. Mater.* **1998**, *10*, 385. c) C. D. Wood, A. I. Cooper, *Macromolecules* **2001**, *34*, 5.
[9] Q. Huo, J. Feng, F. Schüth, G. D. Stucky, *Chem. Mater.* **1997**, *9*, 14.
[10] O. D. Velev, A. M. Lenhoff, E. W. Kaler, *Science* **2000**, *287*, 2240.
[11] G.-R. Yi, J. H. Moon, S.-M. Yang, *Chem. Mater.* **2001**, *13*, 2613.
[12] E. Ruckenstein, L. Hong, *Polymer* **1995**, *36*, 2857.
[13] E. Ruckenstein, L. Hong, *Chem. Mater.* **1996**, *8*, 546.
[14] a) N. R. Cameron, D. C. Sherrington, *Adv. Polym. Sci.* **1996**, *126*, 163. b) E. Ruckenstein, *Adv. Polym. Sci.* **1997**, *127*, 1. c) A. Barbetta, N. R. Cameron, S. J. Cooper, *Chem. Commun.* **2000**, 221.
[15] J. D. Brennan, J. S. Hartman, E. I. Ilnicki, M. Rakic, *Chem. Mater.* **1999**, *11*, 1853.
[16] Mercury intrusion porosimetry measures the size of the pore "windows" between the emulsion templated cells, not the diameter of the cells themselves, which are usually approximately ten times larger.
[17] Y. Miyake, T. Yumoto, H. Kitamura, T. Sugimoto, *Phys. Chem. Chem. Phys.* **2002**, *4*, 2680.

π-Stacked Conjugated Polymers: The Influence of Paracyclophane π-Stacks on the Redox and Optical Properties of a New Class of Broken Conjugated Polythiophenes**

By *Fouad Salhi* and *David M. Collard**

The conductivity of doped conjugated polymers requires the migration of delocalized charge carriers along conjugated chains, and interchain hopping.[1] Cofacial stacking of the conjugated polymer backbones facilitates the latter process. Charge hopping between chains in close contact is also the predominant mode of charge migration in polymers consisting of "broken" conjugated chains.[2] An alternative to the use of self-assembly to obtain cofacial π-systems is to incorporate

[*] Prof. D. M. Collard, Dr. F. Salhi
School of Chemistry and Biochemistry
Georgia Institute of Technology
Atlanta, GA 30332-0400 (USA)
E-mail: david.collard@chemistry.gatech.edu

[**] We thank the National Science Foundation (Award 9501716) for partial support of this research.

  0935-9648/03/0101-0081 $ 17.50+.50/0